Journal of Plant Research (2022) 135:555–564
https://doi.org/10.1007/s10265-022-01401-z

JPR SYMPOSIUM

Regulation of Cyclic Electron Flow, A to Z

Dissection of respiratory and cyclic electron transport in *Synechocystis* sp. PCC 6803

Shoko Kusama[1] · Chikahiro Miyake[2] · Shuji Nakanishi[1] · Ginga Shimakawa[1,3]

Received: 22 December 2021 / Accepted: 1 June 2022 / Published online: 9 June 2022

Abstract

Cyclic electron transport (CET) is an attractive hypothesis for regulating photosynthetic electron transport and producing the additional ATP in oxygenic phototrophs. The concept of CET has been established in the last decades, and it is proposed to function in the progenitor of oxygenic photosynthesis, cyanobacteria. The in vivo activity of CET is frequently evaluated either from the redox state of the reaction center chlorophyll in photosystem (PS) I, P700, in the absence of PSII activity or by comparing PSI and PSII activities through the P700 redox state and chlorophyll fluorescence, respectively. The evaluation of CET activity, however, is complicated especially in cyanobacteria, where CET shares the intersystem chain, including plastoquinone, cytochrome b_6/f complex, plastocyanin, and cytochrome c_6, with photosynthetic linear electron transport (LET) and respiratory electron transport (RET). Here we sought to distinguish the in vivo electron transport rates in RET and CET in the cyanobacterium *Synechocystis* sp. PCC 6803. The reduction rate of oxidized P700 ($P700^+$) decreased to less than 10% when PSII was inhibited, indicating that PSII is the dominant electron source to PSI but $P700^+$ is also reduced by electrons derived from other sources. The oxidative pentose phosphate (OPP) pathway functions as the dominant electron source for RET, which was found to be inhibited by glycolaldehyde (GA). In the condition where the OPP pathway and respiratory terminal oxidases were inhibited by GA and KCN, the $P700^+$ reduction rate was less than 1% of that without any inhibitors. This study indicate that the electron transport to PSI when PSII is inhibited is dominantly derived from the OPP pathway in *Synechocystis* sp. PCC 6803.

Keywords Cyclic electron transport · P700 · Photosynthesis · Photosystem I · Respiratory electron transport

Introduction

Cyanobacteria are photosynthetic prokaryotes that have been considered as the pioneer of oxygenic photosynthesis, in which two important energetic metabolisms, i.e., photosynthesis and respiration, proceed in the same compartment and share many components due to the lack of organelles (Binder 1982; Mullineaux 2014; Peschek et al. 2004; Scherer et al. 1988). The thylakoid membranes in cyanobacterial cells harbour proteins and complexes that function in the electron transport reactions for both energetic metabolisms. In photosynthetic linear electron transport (LET), light energy absorbed at photosystem (PS) II and I drive the photo-oxidation/reduction cycle of the reaction center chlorophylls, P680 and P700 respectively, resulting in the electron transport from H_2O at the luminal side of PSII to $NADP^+$ at the cytosolic side of PSI via the intersystem chain, including plastoquinone (PQ), cytochrome (Cyt) b_6/f complex, plastocyanin, and Cyt c_6. The electron transport through the so-called Q-cycle pumps H^+ into the thylakoid lumen, and the proton motive force thus generated across the membrane leads to production of ATP by the ATP synthase. Therefore, LET mainly functions to produce NADPH

✉ Ginga Shimakawa
ginshimakawa@gmail.com

1 Research Center for Solar Energy Chemistry, Osaka University, 1-3 Machikaneyama, Toyonaka, Osaka 560-8531, Japan

2 Department of Biological and Environmental Science, Faculty of Agriculture, Graduate School of Agricultural Science, Kobe University, 1-1 Rokkodai, Nada, Kobe 657-8501, Japan

3 Department of Bioscience, School of Biological and Environmental Sciences, Kwansei-Gakuin University, 2-1 Gakuen, Sanda, Hyogo 669-1337, Japan

and ATP to assimilate CO_2 in the Calvin-Benson-Bassham (CBB) cycle. Respiratory electron transport (RET) also proceeds in cyanobacterial thylakoid membranes. In cyanobacteria, the oxidative pentose phosphate (OPP) pathway is supposed to function mainly in carbon catabolism (Pelroy and Bassham 1972; Yang et al. 2002) to generate the reductant NADPH to drive RET. In the cyanobacterium *Synechocystis* sp. PCC 6803 (Syn6803), RET at thylakoid membranes is proposed to be initiated by the NAD(P)H dehydrogenase (NDH-1L) complex (Ohkawa et al. 2000) and succinate dehydrogenase (Cooley and Vermaas 2001) that donate electrons to the PQ pool, i.e., the intersystem chain shared with LET. Then, the electrons are finally transferred to O_2 by thylakoidal respiratory terminal oxidases (Lea-Smith et al. 2013), including aa_3-type Cyt *c* oxidase (Cox) and Cyt *bd* quinol oxidase (Cyd). Syn6803 also has alternative respiratory terminal oxidase (ARTO), but it is thought to be located only in the plasma membrane. A certain part of electrons in RET can be transferred to PSI via the shared intersystem chain.

The alternative electron transport pathway from the acceptor side of PSI to PQ is hypothesized to complete cyclic electron transport (CET) around PSI. In cyanobacteria, NDH-1L donates electrons probably from ferredoxin (the electron carrier protein at the cytosolic side of PSI) to PQ (Schuller et al. 2019). The elusive ferredoxin-quinone oxidoreductase is also proposed to be related to CET in photosynthetic eukaryotes but it is still unclear in cyanobacteria. Theoretically, CET proceeds in the light to produce the additional ATP by pumping H^+ to the thylakoid lumen without the accumulation of NADPH. Although numerous previous and recent studies have implicated that CET functions in cyanobacteria (Badger and Schreiber 1993; Dann and Leister 2019; Gao et al. 2016; Mi et al. 1992; Miller et al. 2021; Theune et al. 2021; Yeremenko et al. 2005; Yu et al. 1993), the in vivo CET activity is still controversial.

The electron transport rate through CET estimated indirectly varies widely in each report, which stems from the difficulty to distinguishably analyze the electron transport through PSI from different electron sources in cyanobacteria; this is because LET, RET, and CET share the intersystem components in cyanobacterial thylakoid membranes, resulting in a complicated network of electron transfers. The in vivo activity of cyanobacterial CET has been conventionally evaluated from the reduction rate of the oxidized form of P700 ($P700^+$) upon turning off the actinic light using a near infrared spectrophotometer in the presence of PSII inhibitors such as 3-(3,4-dichlorophenyl)-1,1-dimethylurea (DCMU) (Mi et al. 1992). However, in that condition, the electron flow from the OPP pathway to PSI cannot be excluded (Myers 1987) because the respiratory metabolisms proceed also in the light (Helman et al. 2005; Shimakawa et al. 2021). More concretely, this method qualitatively evaluates the electron transport rate to PSI that depends on the accumulation of electrons in the intersystem chain derived from both light-dependent and -independent electron transport reactions just before the light is turned off. In the light, PQ is reduced by PSII or by cytosolic donors previously reduced by PSI or the OPP pathway. The plastoquinol (PQH_2) can then be oxidized through the activity of PSI or respiratory terminal oxidases, Cox or Cyd. The impaired glycogen degradation decreases the $P700^+$ reduction rate in the presence of DCMU (Shimakawa et al. 2014), indicating the significant electron transfer from the OPP pathway to $P700^+$. If this electron transfer is not taken into account, the electron transfer by cytosolic donors previously reduced by PSI can be over-estimated. Additionally, P700 is kept transiently more reduced at the dark-to-light transition when respiratory terminal oxidases are inhibited or deleted. This is true both with and without DCMU (Bolychevtseva et al. 2015; Shimakawa and Miyake 2018; Viola et al. 2021). The same trend was observed upon the illumination with a strong far-red light (Ermakova et al. 2016). These reports suggest that the significant part of the electron transfer from PQH_2 to PSI can be rerouted to respiratory terminal oxidases. Again, the rate of electron injection into the PQ pool by PSII or cytosolic donors estimated through the $P700^+$ reduction rate would be under-estimated if this rerouting to respiratory oxidases is not considered. To exactly quantify the electron transport activities through PSI originated from different electron donors, we sought to block both electron input and output of RET, i.e., the OPP pathway and respiratory terminal oxidases, in the cyanobacterium Syn6803. We found that the OPP pathway is the dominant electron source for RET and is inhibited by glycolaldehyde (GA) in Syn6803. PSII was inhibited by DCMU, and all three respiratory terminal oxidases were inhibited by KCN or genetically deleted. The decay rate of $P700^+$ was analysed in the wild type cells with and without these inhibitors.

Materials and methods

Cultures

The cyanobacterium Syn6803 was cultured under continuous illumination (30 °C, 100 µmol photons m^{-2} s^{-1}) at 30 °C with constant shaking at 140 rpm in BG-11 medium consisting of the following ingredients (per L): 2 mL of Solution I (0.5 g L^{-1} $Na_2EDTA{\cdot}2H_2O$, 3 g L^{-1} ammonium iron [III] citrate, 3 g L^{-1} citric acid), 25 mL of Solution II-a (60 g L^{-1} $NaNO_3$, 3 g L^{-1} $MgSO_4$), 25 mL of Solution II-b (1.56 g L^{-1} K_2HPO_4), 2 mL of Solution III (14.3 g L^{-1} $CaCl_2$), 1 mL of A6 Solution (2.86 g L^{-1} H_3BO_3, 1.81 g L^{-1} $MnCl_2{\cdot}4H_2O$, 0.22 g L^{-1} $ZnSO_4{\cdot}7H_2O$, 0.08 g L^{-1} $CuSO_4{\cdot}5H_2O$, 0.021 g L^{-1} $Na_2MoO_4{\cdot}H_2O$, 0.0494 g L^{-1} $Co(NO_3)_2{\cdot}6H_2O$, 1

droplet of H_2SO_4), and 20 mL of 1 M TES-KOH (pH 7.5). The mutants of Syn6803 deficient in flavodiiron proteins (FLV) mediating an O_2-dependent alternative electron sink (Δ*flv1/3/4*) and three respiratory terminal oxidases (Δ*cox/cyd/arto*) were previously constructed and cultured like the wild type (Shimakawa et al. 2016, 2021).

Treatments with chemicals

In experiments with inhibitors, Syn6803 cells were harvested centrifugally and resuspended in fresh BG-11 medium, followed by incubation of the following chemicals for at least 30 min: GA (25 mM), iodoacetamide (IA; 8 mM) and KCN (1 mM). In control samples, only solvents (water and dimethylsulfoxide) were added. DCMU was added to the measuring cuvette at the final concentration 5 µM.

Measurement of O_2 exchange

Net O_2 uptake and evolution rates were determined using a closed O_2 electrode (Hansatech, King's Lynn, UK) at 25 °C. The reaction mixture (2 mL) containing fresh BG-11 medium (pH 7.5), 5 mM $NaHCO_3$, and Syn6803 cells treated with or without inhibitors (12 µg chlorophyll mL^{-1}) was stirred with a magnetic microstirrer and illuminated with a CoolLED pE-100 LED (780 µmol photons m^{-2} s^{-1}). The O_2 uptake and evolution rates were calculated from the changes in the O_2 concentration when they reached constant values. In the light, the O_2 evolution rate reached the constant value 3 min after the actinic light was turned on. Chlorophyll *a* was measured in 100% (v/v) methanol spectrophotometrically (Grimme and Boardman 1972). No baseline correction was applied to the measurements.

Measurement of NAD(P)H fluorescence

The in vivo NAD(P)H fluorescence originating from NAD(P)H was measured using the NADPH/9-AA module of a Dual-PAM-100 instrument (Heinz Walz, Effeltrich, Germany) following the method reported in our previous study (Tanaka et al. 2021). The reaction mixture (2 mL) contained fresh BG-11 medium (pH 7.5) and Syn6803 cells (2.4 µg chlorophyll mL^{-1}). The NADPH/9-AA module consisted of an emitter unit (DUAL-ENADPH) and a detector unit (DUAL-DNADPH). NAD(P)H fluorescence was excited by UV-A (365 nm) irradiation from the DUAL-ENADPH unit and was detected using a blue-sensitive photomultiplier with a filter transmitting light between 420 and 580 nm in the DUAL-DNADPH unit. The intensity of the measuring light was on a scale from 1 to 20, and the intensity was set at 10 in the present study. The frequency of the measuring light in the absence and presence of red actinic light (610 µmol photons m^{-2} s^{-1}) was set at 50 and 500 Hz, respectively. No particular normalization was performed.

Measurement of $P700^+$

The transmittance of $P700^+$ was measured using a Dual-PAM-100 (Walz Heinz GmbH, Effeltrich, Germany) at room temperature (25 °C ± 2 °C). The reaction mixture (2 mL) contained fresh BG-11 medium (pH 7.5) and Syn6803 cells (12 µg chlorophyll mL^{-1}). The reduction rate of $P700^+$ was evaluated as the initial rate of the $P700^+$ decay upon turning off the actinic light of various intensities which was illuminated for 10 s. The $P700^+$ signal was defined as zero in the dark since it should be kept fully reduced. For the determination of the maximum oxidation level of P700, termed as P_m, we measured the amplitude of $P700^+$ signal in the 10-s illumination with DCMU. We confirmed that the weak light (30 µmol photons m^{-2} s^{-1}) was even strong enough to fully oxidize P700 in the presence of DCMU. For the analysis of the $P700^+$ decay, we normalized the $P700^+$ signal to the P_m values.

Results

Inhibition of respiration by GA and KCN in Syn6803

To distinguish the activity of CET from that of RET in the wild type cells, the use of respiratory inhibitors is one of the most appropriate methods. In this study, we tested the effects of candidate inhibitors on respiratory and photosynthetic activities in Syn6803. In cyanobacteria, it is well-known that KCN almost completely inhibits respiratory terminal oxidases, including Cox, Cyd, and ARTO (Berry et al. 2002; Pils and Schmetterer 2001; Vermaas et al. 1994). Photosynthetic O_2 evolution is also suppressed by KCN at certain concentrations likely due to the inhibition of ribulose 1,5-bisphosphate carboxylase/oxygenase (Rubisco) (Wang et al. 2012; Wishnick and Lane 1969). These inhibitory effects of KCN were confirmed in the Syn6803 wild type in this study (Table 1). Different from photosynthetic eukaryotes, cyanobacteria are thought to obtain reducing power for driving RET from the OPP pathway (Pelroy and Bassham 1972; Yang et al. 2002). Since the OPP pathway shares most of the enzymatic reactions with the CBB cycle, we assumed that the CBB inhibitors such as GA and IA can inhibit cyanobacterial respiration. Whereas photosynthetic O_2 evolution was inhibited by both inhibitors, respiratory O_2 uptake was suppressed severely with GA but only moderately with IA (Table 1).

To further investigate the inhibitory effects of KCN, GA and IA on cyanobacterial photosynthesis and respiration, we measured the in vivo NAD(P)H fluorescence during the

Table 1 Effects of KCN, GA and IA on O_2 exchange in the Syn6803 wild type

Inhibitors	Net O_2 uptake rate (μmol mg Chl^{-1} h^{-1})	Net O_2 evolution rate (μmol mg Chl^{-1} h^{-1})
No addition	31 ± 9	150 ± 60
KCN	0	20 ± 7
GA	0	17 ± 5
IA	12 ± 4	7 ± 2

Values are shown as the means with the standard deviation ($n = 3$; biological replicates). Inhibitors were added at the following final concentrations: KCN, 1 mM; GA, 25 mM; IA, 8 mM. With KCN or GA, O_2 uptake was not observed at all

light–dark transition in the Syn6803 wild type treated with each inhibitor. Figure 1a shows the typical response of the NAD(P)H fluorescence to a short-term illumination (Feilke et al. 2017; Holland et al. 2015; Mi et al. 2000), which is dominantly derived from the change in the redox state of the photosynthetic NADPH pool (Tanaka et al. 2021). Once the light was turned on, $NADP^+$ was immediately reduced by PSI via ferredoxin and ferredoxin-$NADP^+$ reductase, resulting in the fluorescence induction (Fig. 1a). The fluorescence level was kept high during the illumination with an actinic light. Upon turning off the light, the fluorescence rapidly decreased to the level lower than that before the illumination due to the oxidation of the NADPH pool by glyceraldehyde 3-phosphate dehydrogenase in the CBB cycle (Kauny and Sétif 2014). That is, the photosynthetic NADPH pool was partially kept reduced in the dark before illumination. Furthermore, the post-illumination transient increase of the fluorescence indicated that the $NADP^+$/NADPH pool was transiently more reduced after turning off the light. It has been recently demonstrated that this NADPH reduction in the dark is caused by the OPP pathway (Hatano et al. 2022; Ogawa et al. 2021). In the KCN-treated cells, the NADPH pool was kept highly reduced in the dark as in the light (Fig. 1b), which suggested that the inhibition of the terminal

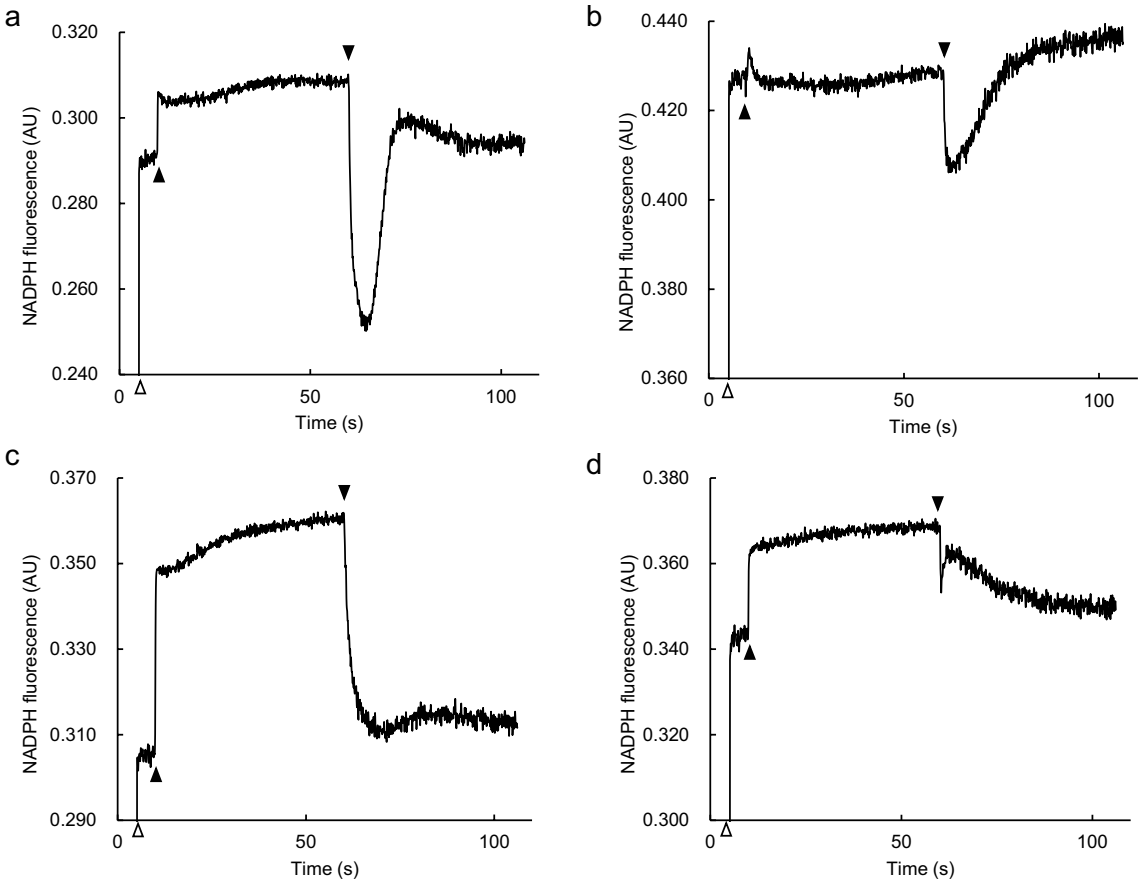

Fig. 1 Changes in the in vivo NAD(P)H fluorescence in the light–dark transition for the Syn6803 wild type without (**a**) and with KCN (**b**), GA (**c**) and IA (**d**). The onset of the measuring light illumination is indicated by white upward triangles; the beginning and the end of the actinic light (610 μmol photons m^{-2} s^{-1}) illumination are indicated by upward and downward black arrows, respectively. Shown are the averaged traces of 3 technical replicates, which are the representative of 3 biological replicates. Inhibitors were added at the following final concentrations: KCN, 1 mM; GA, 25 mM; IA, 8 mM

oxidases accumulated electrons in RET to keep the $NADP^+$/NADPH pool highly reduced; indeed, the same kinetics of the NAD(P)H fluorescence was observed in the mutant Δ*cox/cyd/arto* deficient in all three respiratory terminal oxidases (Fig. S1). After the actinic light was turned off, the re-reduction of $NADP^+$ by the OPP pathway was retarded in the KCN-treated cells (Fig. 1b, Fig. S2d); this is probably due to the inhibition of photosynthetic CO_2 assimilation by KCN, resulting in a decrease in supply CBB cycle intermediates which fuel the OPP pathway (Table 1). Contrary to the KCN-treated cells, the $NADP^+$/NADPH pool was more oxidized in the dark in the GA-treated cells (Fig. 1c). That is, GA inhibited the metabolism to generate NADPH in the dark, i.e., the OPP pathway; this is supported by the experimental result that the Syn6803 mutants impaired in the OPP pathway exhibited more oxidized NAD(P)H pool in the dark (Ogawa et al. 2021) as GA-treated wild-type cells in this study. In the IA-treated wild-type cells, the $NADP^+$/NADPH pool was kept highly reduced after turning off the light, indicating that the oxidation of the photosynthetically generated NADPH was dramatically inhibited (Fig. 1d), which was in agreement with the assumption that IA directly impairs the sulfhydryl group of glyceraldehyde 3-phosphate dehydrogenase (Arnon 1952; Peschek 1978).

We note that the fluorescence decay at the offset of the light was slower in GA-treated wild type cells than in the non-treated ones. On the other hand, the oxidation of the $NADP^+$/NADPH pool was not clearly observed in the IA-treated cells (Fig. S2a–c). This difference between the GA- and IA-treatments would be due to the different inhibition step in the CBB cycle, involving neither NDH-1L complex nor the O_2-dependent alternative electron sink mediated by FLV since the NAD(P)H fluorescence kinetics were similar between the GA-treated wild type, Δ*ndhD*1/2 and Δ*flv*1/*flv*3/*flv*4 mutants (Figs. S3, S4).

Dissection of $P700^+$ reduction originated from PSII and cytosolic electron donors

Based on the experimental results in Table 1 and Fig. 1, the electron input and output of RET are inhibited respectively by GA and KCN, which enables us to estimate the in vivo $P700^+$ reduction by cytosolic electron donors previously reduced by PSI in the Syn6803 wild type whose PSII is inhibited by DCMU. Figure 2 shows the representative traces of the $P700^+$ decay kinetics after 10 s-illumination with the actinic light. In the absence of any inhibitors, $P700^+$ was kept partially reduced during the illumination, and then reduced immediately after turning off the light (Fig. 2). The half time was approximately 16 ± 2 ms (n = 5). In the presence of DCMU, where PSII was completely blocked, the $P700^+$ decay was significantly retarded, and the half time increased to 210 ± 50 ms (n = 5). That is, the reduction of

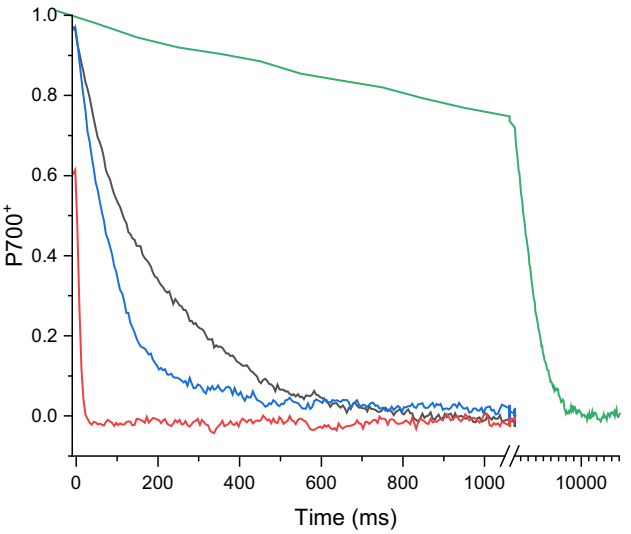

Fig. 2 Changes in the in vivo redox state of P700 upon turning off the actinic light for the Syn6803 wild type without (red) and with DCMU (black), DCMU/KCN (blue) and DCMU/KCN/GA (green). The actinic light (650 µmol photons m^{-2} s^{-1}) was turned off at time zero. Shown are the averaged traces of 3 technical replicates, which is the representative of 3 biological replicates. Inhibitors were added at the following final concentrations: DCMU, 5 µM; KCN, 1 mM; GA, 25 mM

$P700^+$ was mainly derived from PSII. In this situation, the electrons were also transported from the intersystem chain to O_2 via respiratory terminal oxidases, which were inhibited by KCN next. In the presence of both DCMU and KCN, the electrons were supposed to come through NDH-1L as well as through other components, e.g., succinate dehydrogenase, from cytosolic donors previously reduced by the OPP pathway or PSI during the processes of RET and CET (the half time was 100 ± 20 ms; n = 3). In this study, we distinguished the two remaining sources for PQ reduction in the presence of DCMU, i.e., PSI and the OPP pathway, by inhibiting the latter with GA. In the presence of DCMU, KCN and GA, the $P700^+$ decay was dramatically suppressed, and the half time was 3600 ± 700 ms (n = 3), which suggested that the injection of electrons in the intersystem chain is largely dominated by the OPP pathway in the Syn6803 wild type. Further, we analysed the $P700^+$ decay in the mutant Δ*cox/cyd/arto*. The decay of $P700^+$ after the illumination in the presence of DCMU was faster in Δ*cox/cyd/arto* (the half time was 59 ± 6 ms; n = 3) than in the wild type with KCN (Fig. S5), which implied that the abundance of each photosynthetic electron transport component, e.g., PSII, PSI, and the PQ pool size, are different in the mutant from the wild type.

Assuming that the decay of $P700^+$ is the first-order reaction, we simply calculated the rate constant (k) of the $P700^+$ reduction in PSI as $k = \ln 2$/(half time). With a tentative fitting to one-order exponential decay, the relative rate of

$P700^+$ reduction can be expressed with the k value and the amplitude of $P700^+$ signal, $[P700^+]$, as follows:

$$V_{P700} = k \times [P700^+]$$

In this study, we defined the maximum $[P700^+]$, often termed as the total photo-oxidizable P700 (P_m), as 1 to calculate the relative values of V_{P700}. The relative V_{P700} was calculated with each inhibitor set at various light intensities of the actinic light (Table 2). Compared with the OPP pathway, the electron transfer by cytosolic donors reduced by PSI should be strongly dependent on the light intensity. We found that in the presence of DCMU the relative V_{P700} was not affected by light intensity and significantly decreased with GA, which suggested that $P700^+$ was reduced mainly by the light-independent electron transfer by the OPP pathway or that the reduction of cytosolic donors by PSI was already saturated to the light intensity at 30 µmol photon m^{-2} s^{-1} in the tested condition.

Discussion

In this study, we first distinguish the effects of RET and CET on the conventional $P700^+$ reduction analysis in the wild type of cyanobacteria by inhibiting both the input and output of electrons in RET using GA and KCN (Fig. 3). In cyanobacterial thylakoid membranes, LET operates from PSII to PSI, finally producing NADPH; RET proceeds from the OPP pathway or from glycogen degradation to respiratory terminal oxidases, and CET is defined as the electron transport from the acceptor side of PSI to the PQ pool via several proposed pathways (Mi et al. 1992; Yeremenko et al. 2005). Since these electron transport pathways share the intersystem chain, the electrons can be transported from the donor sides of these pathways finally to either PSI or respiratory terminal oxidases (Fig. 3). Previously, we found that the $P700^+$ decay rate was significantly slower in the mutant of Syn6803 impaired in the glycogen degradation (Shimakawa et al. 2014). Degradation of glycogen is critical to the initiation of OPP pathway (Shinde et al. 2020). Further, it was found that the OPP pathway is the dominant source for NADPH related to respiration (Hatano et al. 2022; Ogawa et al. 2021). These findings suggest that the OPP pathway mainly contributes to the $P700^+$ reduction in the presence of DCMU through the reduction of cytosolic electron donors for the intersystem chain. Indeed, the relative V_{P700} decreased to less than 3% by adding GA where PSII and respiratory terminal oxidases were inhibited (Fig. 2; Table 2). The $P700^+$ reduction rate in the absence of DCMU was much higher than that with DCMU (Fig. 2; Table 2), which was in agreement with the experimental finding that LET has significantly larger electron flux than RET as observed in the O_2 evolution and uptake rates (Table 1). Overall, the $P700^+$ decay by cytosolic donors previously reduced by PSI in the process of CET was significantly slower than those by PSII or the OPP pathway, based on the experiments with the inhibitors DCMU, KCN, and GA. Although physiological functions of CET remain to be investigated, its activity should be carefully evaluated in future works especially in cyanobacteria, as originally reported by Myers (1987). It should also be noted that this CET activity may be even over-estimated because we cannot exclude the possibility that other cytosolic reductants slowly donate electrons to the intersystem chain (or directly to PSI) in Syn6803 in the

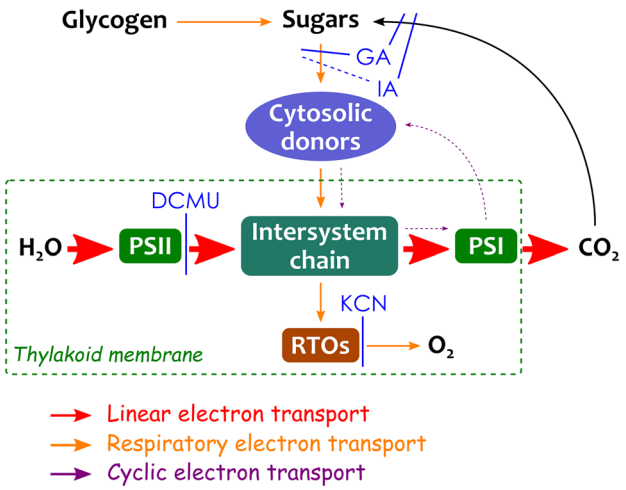

Fig. 3 A schematic diagram of linear, respiratory, and cyclic electron transports in the thylakoid membrane of the Syn6803 wild type. DCMU inhibits PSII, and KCN inhibits RTOs. Both the CBB cycle and OPP pathway are inhibited by GA. IA functions like GA but was not a strong inhibitor to the OPP pathway at the concentration in this study. All abbreviations are spelled out in the text

Table 2 Reduction rate of $P700^+$ (V_{P700}) in the Syn6803 wild type

PFD	−KCN/GA	+KCN	+GA	+KCN/GA
−DCMU				
650	44 ± 5	26 ± 4	57 ± 7	50 ± 6
+DCMU				
30	3.5 ± 1.1	7.5 ± 2	0.18 ± 0.02	0.20 ± 0.04
140	3.6 ± 1.2	7.1 ± 2	0.18 ± 0.02	0.20 ± 0.03
320	3.6 ± 1.0	7.2 ± 1.8	0.18 ± 0.02	0.20 ± 0.03
650	3.5 ± 0.8	7.1 ± 1.5	0.18 ± 0.03	0.20 ± 0.04
1260	3.1 ± 0.4	7.2 ± 1.5	0.17 ± 0.03	0.20 ± 0.04

V_{P700} was calculated as $[P700^+]$ s^{-1}. The absorbance change for $[P700^+]$ was normalized by the maximum amplitude of photo-oxidizable P700 in the Syn6803 wild type as 1. Values are shown as the mean with the standard deviation ($n = 3 \sim 5$; biological replicates). Light intensity is shown as photon flux density (PFD: µmol photons m^{-2} s^{-1}). Inhibitors were added at the following final concentrations: KCN, 1 mM; GA, 25 mM

presence of DCMU, KCN, and GA. Meanwhile, the CET may be under-estimated if the electron supply from PSII and/or the OPP pathway is the limiting step for CET in the experimental condition in this study.

We first characterized the inhibitory effect of GA on the OPP pathway in cyanobacteria. GA is frequently used as an inhibitor to the CBB cycle in a variety of photosynthetic organisms. Although the details of the molecular mechanism have not been fully understood, the plausible target enzyme is phosphoribulokinase that catalyses phosphorylation of ribulose 5-phosphate (Gardeström and Wigge 1988; Sicher 1984; Takahashi and Murata 2006). Therefore, the NADPH-oxidation step in the CBB cycle is unlikely to be the exact limitation step in the GA-inhibited photosynthesis, which is consistent with the result that the NAD(P)H fluorescence showed the decay upon turning off the light in the GA-treated wild type and the mutant deficient in FLV (Fig. 1c, Fig. S4). It remains to be uncovered how the OPP pathway was inhibited by GA. A downregulation of phosphoribulokinase in tobacco leaves leads to overaccumulation of ribulose 5-phosphate (Ru5P) (Paul et al. 1995). Therefore, inhibition of 6-phosphogluconate dehydrogenase by the accumulated Ru5P (Ito and Osanai 2018) may occur in the presence of GA, leading to suppression of the OPP pathway. Meanwhile, GA inhibits ethanol fermentation in *Saccharomyces cerevisiae* (Jayakody et al. 2011), which is devoid of phosphoribulokinase; this suggests that, with its high reactivity (Adrover et al. 2008; Glomb and Monnier 1995; Hayashi and Namiki 1986), GA might directly interact with proteins involved in the OPP pathway. Different from GA, IA directly inhibited the NADPH-oxidation reaction by glyceraldehyde 3-phosphate dehydrogenase in the CBB cycle (Arnon 1952; Peschek 1978) and did not affect the respiratory O_2 uptake as strongly as GA (Table 1).

KCN is a well-known inhibitor to respiratory terminal oxidases, and the inhibitory effect has been confirmed in cyanobacteria in previous studies (Berry et al. 2002; Pils and Schmetterer 2001; Vermaas et al. 1994). In this study, we found the accumulation of NADPH in the dark by 1 mM KCN, confirming its inhibitory effect on the terminal oxidases (Fig. 1b). Meanwhile, it is also known that KCN inhibits other components as follows. KCN inhibits catalase even at low concentrations (> 60 µM) (Allen and Hall 1974; Allen and Whatley 1978). However, the catalase activity is unlikely to affect the quantitative evaluation of $P700^+$ reduction rate in this study. The CBB cycle enzyme Rubisco, and the soluble electron donor for PSI, plastocyanin, can also be inhibited by KCN (Katoh 1960; Ouitrakul and Izawa 1973; Wishnick and Lane 1969), which is consistent with the suppressed O_2 evolution rate (Table 1). Judging from the fact that plastocyanin is inhibited by KCN only at a high concentration (> 10 mM) (Izawa et al. 1973; Ouitrakul and Izawa 1973), and the increase in V_{P700} in the presence of DCMU and KCN (Fig. 2; Table 2), we concluded that plastocyanin was not severely inhibited in our experimental setup. Meanwhile, V_{P700} was significantly decreased by KCN in the absence of DCMU (Table 2). Although the exact inhibitory mechanism is not yet verified, it is possible that the highly reduced PQ pool by KCN stimulates state transition (Mullineaux and Allen 1986) to partially suppress the photo-excitation of PSII in the absence of DCMU. In this study, we further analysed the $P700^+$ decay in the presence of each inhibitor in the mutant Δ*cox/cyd/arto*. Surprisingly, Δ*cox/cyd/arto* showed faster decay of $P700^+$ in the measurement (Fig. S5), implying that the amounts and/or pool size of photosynthetic components are changed by the deletion of respiration. Indeed, the amplitude corresponding to the total photo-oxidizable P700 based on the chlorophyll content was slightly smaller in Δ*cox/cyd* than in the wild type (Shimakawa and Miyake 2018). The photosynthetic parameters in respiratory mutants should be carefully interpreted in cyanobacteria.

Here we summarize the problems in the evaluation of CET from in vivo P700 measurement in cyanobacteria, some of which were solved in this study but others still remain unclear. The $P700^+$ decay analysis with DCMU has been conventionally used for the estimation of in vivo CET activity (Mi et al. 1992; Myers 1987; Yeremenko et al. 2005). This method has several advantages to measure in vivo electron transport activity into PSI. In the presence of DCMU, the PQ pool should be kept oxidized and the distribution of the excitation between PSII and PSI (i.e., state transition) is fixed to state I where PSII is preferentially excited (Kirilovsky 2015; Mullineaux and Allen 1986). Additionally, there is no acceptor-side limitation, which is highly likely to suppress the contribution of charge recombination to $P700^+$ reduction (Milanovsky et al. 2019). Meanwhile, we note that the $P700^+$ reduction rate, i.e., V_{P700}, does not exactly indicate the electron flux into PSI because of the fast redox equilibration among Cyt *f*, plastocyanin and PSI (the so-called high potential chain) (Furutani et al. 2020; Oja et al. 2003; Sacksteder and Kramer 2000; Theune et al. 2021). As recently reported by Theune et al. (2021), the quantitative evaluation of the electron flux into PSI needs comprehensive analysis for the reduction of the high potential chain in cyanobacteria. In this study, we compared the $P700^+$ decay related to RET and CET in the presence of DCMU, where the high potential chain should be kept oxidized in all measurements. While avoiding the use of respiratory mutants, the simultaneous presence of DCMU, GA and KCN led to inhibition of the electron input from both PSII and the OPP pathway as well as output to respiratory terminal oxidases in the wild type of Syn6803. As a result, we found that, in the absence of PSII activity, the electron injection to the intersystem chain is dominantly originated from the OPP pathway in Syn6803. It is not yet understood

to what extent CET functions under the conditions where all the components of electron transport chains operate properly, since there is no method validated to estimate the CET activity without any inhibitors or mutants except for the one described in the latest work by Theune et al. (2021), which could not fully solve the "intersystem chain problem" in cyanobacteria. Therefore, the inhibitory effects on either LET or RET might cause under- or over-estimation of the in vivo CET activity. Indeed, the addition of DCMU has been reported to change the distribution of NDH-1L complex (Liu et al. 2012). We note that the activity of RET was even possibly under-estimated in the presence of DCMU because the OPP pathway is driven by the substrates that are produced in photosynthetic CO_2 assimilation.

Supplementary Information The online version contains supplementary material available at https://doi.org/10.1007/s10265-022-01401-z.

Acknowledgements We thank Dr. Ohkawa (Hirosaki University) and Prof. K. Sonoike (Waseda University) for kindly providing the mutant Δ*ndhD*1/2 used in this work.

Author contributions GS conceived the research plans; SK performed all experiments with the technical assistance from GS; SK and GS designed the experiments. All the authors analysed the data and wrote the manuscript.

Funding This work was supported by the Japan Society for the Promotion of Science (JSPS; Grant no. 21399224 to GS).

Declarations

Conflict of interest The authors have no conflict of interest to declare.

References

Adrover M, Vilanova B, Muñoz F, Donoso J (2008) Kinetic study of the reaction of glycolaldehyde with two glycation target models. Ann NY Acad Sci 1126:235–240

Allen JF, Hall DO (1974) The relationship of oxygen uptake to electron transport in photosystem I of isolated chloroplasts: the role of superoxide and ascorbate. Biochem Biophys Res Commun 58:579–585

Allen JF, Whatley FR (1978) Effects of inhibitors of catalase on photosynthesis and on catalase activity in unwashed preparations of intact chloroplasts. Plant Physiol 61:957–960

Arnon D (1952) The glycolytic cycle in the breakdown and synthesis of carbohydrates in green leaves. Phosphorus Metab 2:67–79

Badger MR, Schreiber U (1993) Effects of inorganic carbon accumulation on photosynthetic oxygen reduction and cyclic electron flow in the cyanobacterium *Synechococcus* PCC7942. Photosynth Res 37:177–191

Berry S, Schneider D, Vermaas WFJ, Rögner M (2002) Electron transport routes in whole cells of *Synechocystis* sp. Strain PCC 6803: the role of the cytochrome *bd*-type oxidase. Biochemistry 41:3422–3429

Binder A (1982) Respiration and photosynthesis in energy-transducing membranes of cyanobacteria. J Bioenerg Biomembr 14:271–286

Bolychevtseva YV, Kuzminov FI, Elanskaya IV, Gorbunov MY, Karapetyan NV (2015) Photosystem activity and state transitions of the photosynthetic apparatus in cyanobacterium *Synechocystis* PCC 6803 mutants with different redox state of the plastoquinone pool. Biochem Mosc 80:50–60

Cooley JW, Vermaas WFJ (2001) Succinate dehydrogenase and other respiratory pathways in thylakoid membranes of *Synechocystis* sp. strain PCC 6803: capacity comparisons and physiological function. J Bacteriol 183:4251–4258

Dann M, Leister D (2019) Evidence that cyanobacterial Sll1217 functions analogously to PGRL1 in enhancing PGR5-dependent cyclic electron flow. Nat Commun 10:5299

Ermakova M, Huokko T, Richaud P, Bersanini L, Howe CJ, Lea-Smith DJ, Peltier G, Allahverdiyeva Y (2016) Distinguishing the roles of thylakoid respiratory terminal oxidases in the cyanobacterium *Synechocystis* sp. PCC 6803. Plant Physiol 171:1307–1319

Feilke K, Ajlani G, Krieger-Liszkay A (2017) Overexpression of plastid terminal oxidase in *Synechocystis* sp. PCC 6803 alters cellular redox state. Philos Trans R Soc B Biol Sci 372:20160379

Furutani R, Ifuku K, Suzuki Y, Noguchi K, Shimakawa G, Wada S, Makino A, Sohtome T, Miyake C (2020) P700 oxidation suppresses the production of reactive oxygen species in photosystem I. In: Hisabori T (ed) Advances in botanical research, vol 96. Academic Press, Cambridge, pp 151–176

Gao F, Zhao J, Chen L, Battchikova N, Ran Z, Aro E-M, Ogawa T, Ma W (2016) The NDH-1L-PSI supercomplex is important for efficient cyclic electron transport in cyanobacteria. Plant Physiol 172:1451–1464

Gardeström P, Wigge B (1988) Influence of photorespiration on ATP/ADP ratios in the chloroplasts, mitochondria, and cytosol, studied by rapid fractionation of barley (*Hordeum vulgare*) protoplasts 1. Plant Physiol 88:69–76

Glomb MA, Monnier VM (1995) Mechanism of protein modification by glyoxal and glycolaldehyde, reactive intermediates of the maillard reaction. J Biol Chem 270:10017–10026

Grimme LH, Boardman NK (1972) Photochemical activities of a particle fraction P_1 obtained from the green alga *Chlorella fusca*. Biochem Biophys Res Commun 49:1617–1623

Hatano J, Kusama S, Tanaka K, Kohara A, Miyake C, Nakanishi S, Shimakawa G (2022) NADPH production in dark stages is critical for cyanobacterial photocurrent generation: a study using mutants deficient in oxidative pentose phosphate pathway. Photosynth Res (**in press**)

Hayashi T, Namiki M (1986) Role of sugar fragmentation in an early stage browning of amino-carbonyl reaction of sugar with amino acid. Agric Biol Chem 50:1965–1970

Helman Y, Barkan E, Eisenstadt D, Luz B, Kaplan A (2005) Fractionation of the three stable oxygen isotopes by oxygen-producing and oxygen-consuming reactions in photosynthetic organisms. Plant Physiol 138:2292–2298

Holland SC, Kappell AD, Burnap RL (2015) Redox changes accompanying inorganic carbon limitation in *Synechocystis* sp. PCC 6803. Biochim Biophys Acta Bioenerg 1847:355–363

Ito S, Osanai T (2018) Single amino acid change in 6-phosphogluconate dehydrogenase from *Synechocystis* conveys higher affinity for $NADP^+$ and altered mode of inhibition by NADPH. Plant Cell Physiol 59:2452–2461

Izawa S, Kraayenhof R, Ruuge E, Devault D (1973) The site of KCN inhibition in the photosynthetic electron transport pathway. Biochim Biophys Acta Bioenerg 314:328–339

Jayakody LN, Hayashi N, Kitagaki H (2011) Identification of glycolaldehyde as the key inhibitor of bioethanol fermentation by yeast and genome-wide analysis of its toxicity. Biotechnol Lett 33:285–292

Katoh S (1960) A new copper protein from *Chlorella ellipsoidea*. Nature 186:533–534

Kauny J, Sétif P (2014) NADPH fluorescence in the cyanobacterium *Synechocystis* sp. PCC 6803: a versatile probe for in vivo measurements of rates, yields and pools. Biochim Biophys Acta Bioenerg 1837:792–801

Kirilovsky D (2015) Modulating energy arriving at photochemical reaction centers: orange carotenoid protein-related photoprotection and state transitions. Photosynth Res 126:3–17

Lea-Smith DJ, Ross N, Zori M, Bendall DS, Dennis JS, Scott SA, Smith AG, Howe CJ (2013) Thylakoid terminal oxidases are essential for the cyanobacterium *Synechocystis* sp. PCC 6803 to survive rapidly changing light intensities. Plant Physiol 162:484–495

Liu L-N, Bryan SJ, Huang F, Yu J, Nixon PJ, Rich PR, Mullineaux CW (2012) Control of electron transport routes through redox-regulated redistribution of respiratory complexes. Proc Natl Acad Sci USA 109:11431–11436

Mi H, Endo T, Schreiber U, Ogawa T, Asada K (1992) Electron donation from cyclic and respiratory flows to the photosynthetic intersystem chain is mediated by pyridine nucleotide dehydrogenase in the cyanobacterium *Synechocystis* PCC 6803. Plant Cell Physiol 33:1233–1237

Mi H, Klughammer C, Schreiber U (2000) Light-induced dynamic changes of NADPH fluorescence in *Synechocystis* PCC 6803 and its *ndhB*-defective mutant M55. Plant Cell Physiol 41:1129–1135

Milanovsky G, Gopta O, Petrova A, Mamedov M, Gorka M, Cherepanov D, Golbeck JH, Semenov A (2019) Multiple pathways of charge recombination revealed by the temperature dependence of electron transfer kinetics in cyanobacterial photosystem I. Biochim Biophys Acta Bioenerg 1860:601–610

Miller NT, Vaughn MD, Burnap RL (2021) Electron flow through NDH-1 complexes is the major driver of cyclic electron flow-dependent proton pumping in cyanobacteria. Biochim Biophys Acta Bioenerg 1862:148354

Mullineaux CW (2014) Co-existence of photosynthetic and respiratory activities in cyanobacterial thylakoid membranes. Biochim Biophys Acta Bioenerg 1837:503–511

Mullineaux CW, Allen JF (1986) The state 2 transition in the cyanobacterium *Synechococcus* 6301 can be driven by respiratory electron flow into the plastoquinone pool. FEBS Lett 205:155–160

Myers J (1987) Is there significant cyclic electron flow around photoreaction 1 in cyanobacteria? Photosynth Res 14:55–69

Ogawa T, Suzuki K, Sonoike K (2021) Respiration interacts with photosynthesis through the acceptor side of photosystem I, reflected in the dark-to-light induction kinetics of chlorophyll fluorescence in the cyanobacterium *Synechocystis* sp. PCC 6803. Front Plant Sci 12

Ohkawa H, Pakrasi HB, Ogawa T (2000) Two types of functionally distinct NAD(P)H dehydrogenases in *Synechocystis* sp. Strain PCC6803. J Biol Chem 275:31630–31634

Oja V, Eichelmann H, Peterson RB, Rasulov B, Laisk A (2003) Deciphering the 820 nm signal: redox state of donor side and quantum yield of Photosystem I in leaves. Photosynth Res 78:1

Ouitrakul R, Izawa S (1973) Electron transport and photophosphorylation in chloroplasts as a function of the electron acceptor. II. Acceptor-specific inhibition by KCN. Biochim Biophys Acta Bioenerg 305:105–118

Paul MJ, Knight JS, Habash D, Parry MAJ, Lawlor DW, Barnes SA, Loynes A, Gray JC (1995) Reduction in phosphoribulokinase activity by antisense RNA in transgenic tobacco: effect on CO_2 assimilation and growth in low irradiance. Plant J 7:535–542

Pelroy RA, Bassham JA (1972) Photosynthetic and dark carbon metabolism in unicellular blue-green algae. Arch Mikrobiol 86:25–38

Peschek GA (1978) Reduced sulfur and nitrogen compounds and molecular hydrogen as electron donors for anaerobic CO_2 photoreduction in *Anacystis nidulans*. Arch Microbiol 119:313–322

Peschek GA, Obinger C, Paumann M (2004) The respiratory chain of blue-green algae (cyanobacteria). Physiol Plant 120:358–369

Pils D, Schmetterer G (2001) Characterization of three bioenergetically active respiratory terminal oxidases in the cyanobacterium *Synechocystis* sp. strain PCC 6803. FEMS Microbiol Lett 203:217–222

Sacksteder CA, Kramer DM (2000) Dark-interval relaxation kinetics (DIRK) of absorbance changes as a quantitative probe of steady-state electron transfer. Photosynth Res 66:145–158

Scherer S, Almon H, Böger P (1988) Interaction of photosynthesis, respiration and nitrogen fixation in cyanobacteria. Photosynth Res 15:95–114

Schuller JM, Birrell JA, Tanaka H, Konuma T, Wulfhorst H, Cox N, Schuller SK, Thiemann J, Lubitz W, Sétif P, Ikegami T, Engel BD, Kurisu G, Nowaczyk MM (2019) Structural adaptations of photosynthetic complex I enable ferredoxin-dependent electron transfer. Science 363:257–260

Shimakawa G, Miyake C (2018) Respiratory terminal oxidases alleviate photo-oxidative damage in photosystem I during repetitive short-pulse illumination in *Synechocystis* sp. PCC 6803. Photosynth Res 137:241–250

Shimakawa G, Hasunuma T, Kondo A, Matsuda M, Makino A, Miyake C (2014) Respiration accumulates Calvin cycle intermediates for the rapid start of photosynthesis in *Synechocystis* sp. PCC 6803. Biosci Biotechnol Biochem 78:1997–2007

Shimakawa G, Shaku K, Miyake C (2016) Oxidation of P700 in photosystem I is essential for the growth of cyanobacteria. Plant Physiol 172:1443–1450

Shimakawa G, Kohara A, Miyake C (2021) Characterization of light-enhanced respiration in cyanobacteria. Int J Mol Sci 22:342

Shinde S, Zhang X, Singapuri SP, Kalra I, Liu X, Morgan-Kiss RM, Wang X (2020) Glycogen metabolism supports photosynthesis start through the oxidative pentose phosphate pathway in cyanobacteria. Plant Physiol 182:507–517

Sicher RC (1984) Glycolaldehyde inhibition of photosynthetic carbon assimilation by isolated chloroplasts and protoplasts. In: Sybesma C (ed) Advances in photosynthesis research, vol 3. Springer, Berlin, pp 413–416

Takahashi S, Murata N (2006) Glycerate-3-phosphate, produced by CO_2 fixation in the Calvin cycle, is critical for the synthesis of the D1 protein of photosystem II. Biochim Biophys Acta Bioenerg 1757:198–205

Tanaka K, Shimakawa G, Tabata H, Kusama S, Miyake C, Nakanishi S (2021) Quantification of NAD(P)H in cyanobacterial cells by a phenol extraction method. Photosynth Res 148:57–66

Theune ML, Hildebrandt S, Steffen-Heins A, Bilger W, Gutekunst K, Appel J (2021) In-vivo quantification of electron flow through photosystem I—cyclic electron transport makes up about 35% in a cyanobacterium. Biochim Biophys Acta Bioenerg 1862:148353

Vermaas WFJ, Shen G, Styling S (1994) Electrons generated by photosystem II are utilized by an oxidase in the absence of photosystem I in the cyanobacterium *Synechocystis* sp. PCC 6803. FEBS Lett 337:103–108

Viola S, Sellés J, Bailleul B, Joliot P, Wollman F-A (2021) In vivo electron donation from plastocyanin and cytochrome c_6 to PSI in *Synechocystis* sp. PCC6803. Biochim Biophys Acta Bioenerg 148449

Wang QJ, Singh A, Li H, Nedbal L, Sherman LA, Govindjee WJ (2012) Net light-induced oxygen evolution in photosystem I deletion mutants of the cyanobacterium *Synechocystis* sp. PCC 6803. Biochim Biophys Acta Bioenerg 1817:792–801

Wishnick M, Lane MD (1969) Inhibition of ribulose diphosphate carboxylase by cyanide: inactive ternary complex of enzyme, ribulose diphosphate, and cyanide. J Biol Chem 244:55–59

Yang C, Hua Q, Shimizu K (2002) Metabolic flux analysis in *Synechocystis* using isotope distribution from 13C-labeled glucose. Metab Eng 4:202–216

Yeremenko N, Jeanjean R, Prommeenate P, Krasikov V, Nixon PJ, Vermaas WFJ, Havaux M, Matthijs HCP (2005) Open reading

frame ssr2016 is required for antimycin A-sensitive photosystem I-driven cyclic electron flow in the cyanobacterium *Synechocystis* sp. PCC 6803. Plant Cell Physiol 46:1433–1436

Yu L, Zhao J, Muhlenhoff U, Bryant DA, Golbeck JH (1993) Psae is required for in vivo cyclic electron flow around photosystem i in the cyanobacterium *Synechococcus* sp. PCC 7002. Plant Physiol 103:171–180